Journal of Alloys and Compounds 499 (2010) 171–175

Contents lists available at ScienceDirect

Journal of Alloys and Compounds

journal homepage: www.elsevier.com/locate/jallcom

High-temperature microstructural characteristics of a novel biomedical titanium alloy

Ming-Chih Chang[a,b,c], Chin-Wan Luo[c,d,1], Mao-Suan Huang[c,d], Keng-Liang Ou[c,e,f,**], Li-Hsiang Lin[c,g,h], Hsin-Chung Cheng[c,g,h,*]

[a] Department of Dentistry, Cathay General Hospital, Taipei 106, Taiwan
[b] Department of Dentistry, Sijhih Cathay General Hospital, Taipei 221, Taiwan
[c] Research Center for Biomedical Devices, Taipei Medical University, Taipei 110, Taiwan
[d] Department of Dentistry, Taipei Medical University-Shuang Ho Hospital, Taipei 235, Taiwan
[e] Research Center for Biomedical Implants and Microsurgery Devices, Taipei Medical University, Taipei 110, Taiwan
[f] Graduate Institute of Biomedical Materials and Engineering, Taipei Medical University, Taipei 110, Taiwan
[g] Department of Dentistry, Taipei Medical University Hospital, Taipei 110, Taiwan
[h] School of Dentistry, College of Oral Medicine, Taipei Medical University, Taipei 110, Taiwan

ARTICLE INFO

Article history:
Received 18 January 2010
Received in revised form 23 February 2010
Accepted 2 March 2010
Available online 9 March 2010

Keywords:
Titanium alloy
High-temperature microstructure
Transmission electron microscopey
Phase transformation

ABSTRACT

In this study, the high-temperature microstructural characteristics of the Ti–5Al–1Sn–1Fe–1Cr (Ti-5111) alloy were determined by optical microscopy, scanning electron microscopy, transmission electron microscopy, and energy-dispersive X-ray spectrometry. During solution treatment between 800 and 1000 °C, the phase transformation sequence of the alloy was found to be $(\alpha+\beta)\rightarrow(\alpha+\alpha'+\beta)\rightarrow(\alpha+\alpha'+\alpha''+\text{residual }\beta)\rightarrow(\alpha'+\beta)$. The residual β phase subsequently transforms to the α″ phase during quenching. The driving force for this transformation is the cooling rate. The martensite starting point (Ms) and β transus temperature of the Ti-5111 alloy are nearly 860 and 960 °C, respectively. These values are lower than those of the Ti–6Al–4V alloy. Moreover, it is believed that the concentration of Al in α′ martensite plays a crucial role in the formation of the twin-type martensite.

1. Introduction

Titanium (Ti) and its alloys possess a unique combination of physical and biological properties such as high strength and stiffness, low density, good corrosion and oxidation resistance, and excellent biocompatibility [1–9]. Hence, they are extensively used in a variety of aerospace, chemical, and biomedical applications. Duplex (α + β)-phase Ti–6Al–4V has been the main alloy used in biomedical applications for a long period, because it combines high strength with workability, and duplex alloys are usually thermomechanically processed or heat treated to refine the microstructure and tailor the mechanical properties to the desired application. However, recent studies have shown that the Ti–6Al–4V alloy has low wear resistance [10] and a relatively high elasticity modulus than bone [11]. Thus, novel Ti-based alloys such as Ti–15Mo [1], Ti–13Nb–13Zr [2], Ti–35Nb–2Ta–3Zr [12], Ti–Mo–Nb [13], and Ti–50Ta [14] have been developed as potential materials for biomedical uses such as dental implants, bone plates, crowns, artificial vascular stents, and screws for fracture fixation [15–18].

From a financial point of view, it would be desirable if expensive alloying elements such as V, Zr, Nb, Ta, and Mo could be replaced with cheaper elements without sacrificing desirable mechanical and biological properties. Accordingly, new alloys with high strength and low cost are being developed, e.g., Ti–Si [19], Ti–Fe–Si [20], Ti–Al–Fe [21], and Ti–Fe–Sn [3]. Recently, we have focused on the duplex Ti-5111 alloy because of its price advantage and attractive properties. In the Ti-5111 alloy system, Al stabilizes the α phase and improves the corrosion and oxidation resistance behavior. Fe is known to be a low-cost β phase stabilizer [20,21]. Cr addition can promote the plasticity of duplex alloys and increases the tendency of Ti to passivate [22]. The addition of Sn increases solution strengthening and enhances biocompatibility. In addition, Hsu et al. [23] pointed out that Ti with (1 wt.%) Sn alloy had the most favorable mechanical properties, making it the best candidate for prosthetic dental applications. It is generally concluded that the Ti-5111 alloy possesses excellent properties such as high specific strength, good corrosion and oxidation resistance, superior workability, and good biocompatibility. Thus, it is a potential material for implants and dental orthodontic devices.

* Corresponding author at: Research Center for Biomedical Devices, Taipei Medical University, Taipei 110, Taiwan. Tel.: +886 2 27361661x5400; fax: +886 2 27395524.
** Co-corresponding author.
E-mail address: g4808@tmu.edu.tw (H.-C. Cheng).
[1] Co-first author.

0925-8388/$ – see front matter © 2010 Published by Elsevier B.V.
doi:10.1016/j.jallcom.2010.03.052

It is well known that the microstructures and mechanical properties of Ti alloy are closely related to the hot working history of the alloy. Understanding the high-temperature microstructure transition behavior is of great importance in the isothermal forging and superplasticity formation of a new duplex Ti alloy. Therefore, the purpose of the present study is to investigate the high-temperature microstructural characteristics of the Ti-5111 alloy and thus provide information that would be valuable in biomedical applications.

2. Experimental procedures

The alloy of interest was prepared in a vacuum arc remelting furnace with a non-consumable W electrode and a water-cooled copper hearth under a protective N_2 atmosphere using high-purity sponge titanium, 99.7%-pure electrolytic Al, AISI 1008 low-carbon steel, pure Sn, and pure Cr. The ingot was remelted three times to ensure compositional homogeneity. The button ingot was nearly 1.5 kg in mass. The chemical composition of the investigated alloy determined by inductively coupled plasma-atomic emission spectrometry was Ti–5.07Al–0.95Sn–0.92Fe–1.13Cr–0.006C–0.004N–0.006O (wt.%). After homogenization at 1000 °C for 4 h in a protective Ar atmosphere, the ingot was hot forged and cold rolled to a sheet with a final thickness of 2.5 mm.

Solution treatment was conducted at temperatures ranging from 800 to 1000 °C for 30 min in a vacuum furnace, and this was followed by rapid quenching to room temperature in water. The specimens for optical microscopy (Olympus BX-51) and scanning electron microscopy (SEM; JEOL JSM-6500F) were abraded with SiC paper, polished with 0.3 μm Al_2O_3 powder, washed in distilled water, ultrasonically degreased in acetone, and etched with a mixture of 3 ml HF, 5 ml HNO_3, and 92 ml H_2O. The percentage volume of each phase was measured using an image analyzer (Buehler OmniMet); the average of 10 tests was considered. Transmission electron microscopy (TEM) was conducted using a Philips-CM200 operated at 200 kV. Elemental distributions were examined by energy-dispersive X-ray spectrometry (EDS). The average weight percentages of alloying elements were examined by analyzing at least 10 different EDS spectra of each phase. Samples for TEM were prepared by mechanical grinding to 30 μm thickness and electropolishing with an electrolyte containing 300 ml methyl alcohol, 170 ml *n*-butyl alcohol, and 30 ml perchloric acid at a current density of $1.5–2.5 \times 10^4$ A/m^2 at a temperature less than −15 °C.

3. Results and discussion

Fig. 1(a)–(f) shows the optical micrographs of the Ti-5111 alloy solution-treated at various temperatures for 30 min. After the investigated alloy was solution-treated at 800 °C for 30 min, it had a typical dual-phase microstructure, as shown in Fig. 1(a). It is clearly seen that the alloy contained fine island-like phases dispersed in the matrix. The microstructural characteristic was similar to that of the common Ti–6Al–4V alloy [24]. The same structure was also observed at temperatures between 830 and 860 °C, as shown in Fig. 1(b) and (c). Only the grain sizes of the island-like phase slightly changed with temperature. The average grain sizes of the island-like phase in the samples solution-treated at 800, 830, and 860 °C for 30 min were determined using an image analyzer and found to be approximately 18.6, 25.5, and 32.1 μm, respectively. When the investigated alloy was solution-treated at 890 °C for 30 min, precipitates formed in the matrix and on the grain boundaries, as illustrated in Fig. 1(d). As the temperature increased to 920 °C, there were no significant differences in the microstructure as compared with Fig. 1(d). The grain size of the matrix phase slightly increased with temperature, as depicted in Fig. 1(e). It is clearly seen that the precipitate has a needle-like morphology in the matrix. When the alloy was solution-treated at 960 °C for 30 min, the microstructure changed to a single-phase structure, as shown in Fig. 1(f). Above 960 °C, the microstructure was the same as that seen in Fig. 1(f).

Electron microscopy observations revealed that no other precipitates were formed in the investigated alloy after solution treatment at temperatures between 800 and 830 °C. However, some acicular precipitates formed in the matrix of the alloy solution-treated at 860 °C. Fig. 2(a) is a bright field (BF) image of the [0 1 1] zone of the island-like phase, which was taken from the matrix in Fig. 1(c). The image indicates that the island-like phase is a β phase with body-center-cubic (BCC) structure [25]. Fig. 2(b) depicts a [1 1 $\bar{2}$ 0] selected-area electron diffraction pattern (SAEDP) taken from the matrix in Fig. 1(c) and reveals that the matrix is an α phase with a hexagonal-close-packed (HCP) structure. In addition to the reflection spots of the α phase, the SAEDP also contains small superlattice spots. From the camera length and *d*-spacings of the superlattice spots, it is concluded that the spots were α′ martensites having an HCP structure and lattice parameters $a = 2.93$ nm and $c = 4.66$ nm [4,26]. Fig. 2(c) shows the α′ martensite dark field (DF) image; this image clearly shows the presence of the α′ martensite in the matrix. Moreover, a high density of dislocations is observed within the α′ martensite. The α′ martensite

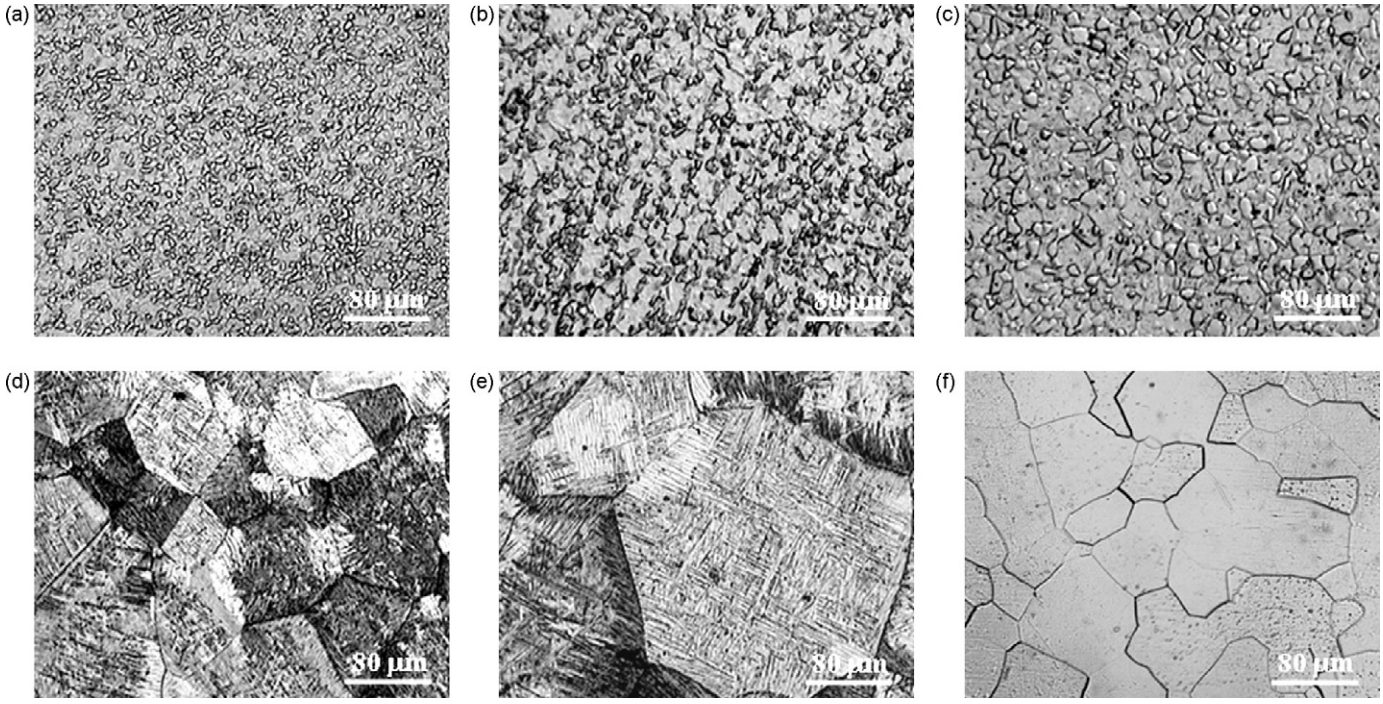

Fig. 1. Optical micrographs of the Ti-5111 alloy samples underwent solution-treated at (a) 800 °C, (b) 830 °C, (c) 860 °C, (d) 890 °C, (e) 920 °C and (f) 960 °C for 30 min.

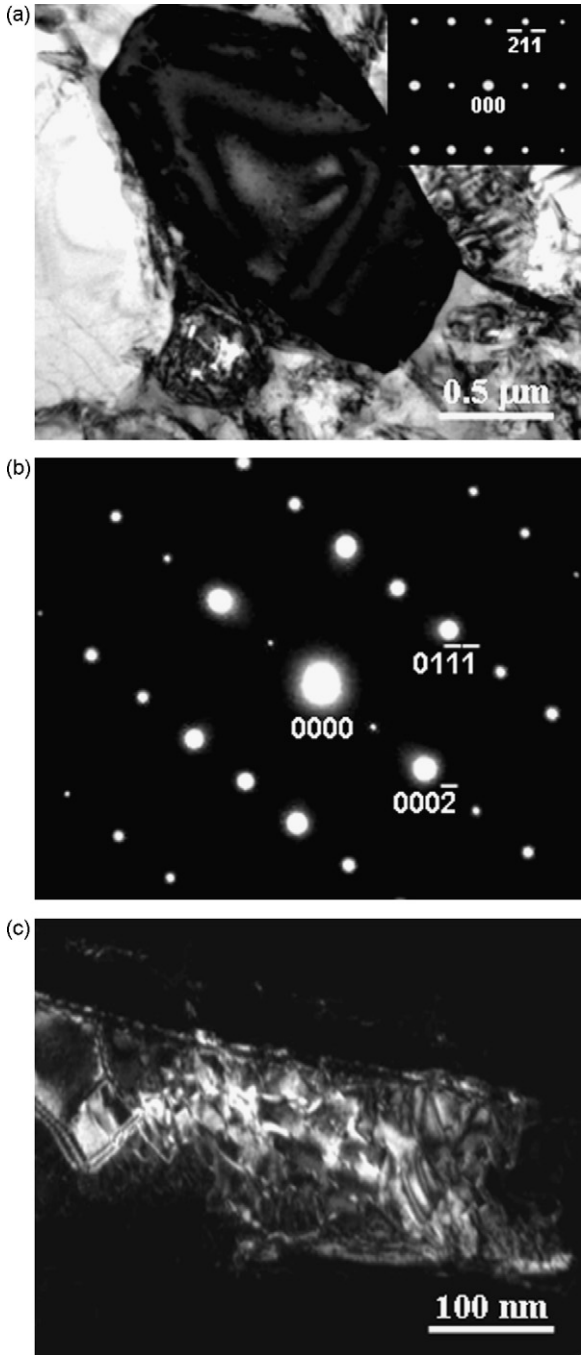

Fig. 2. TEM micrographs of the Ti-5111 alloy sample underwent solution-treated at 860 °C for 30 min: (a) a BF image of the [0 1 1] zone of the island-like phase, (b) a [1 $1\ \bar{2}\ 0$] SAEDP taken from the matrix in Fig. 1(c), and (c) the α′ martensite DF.

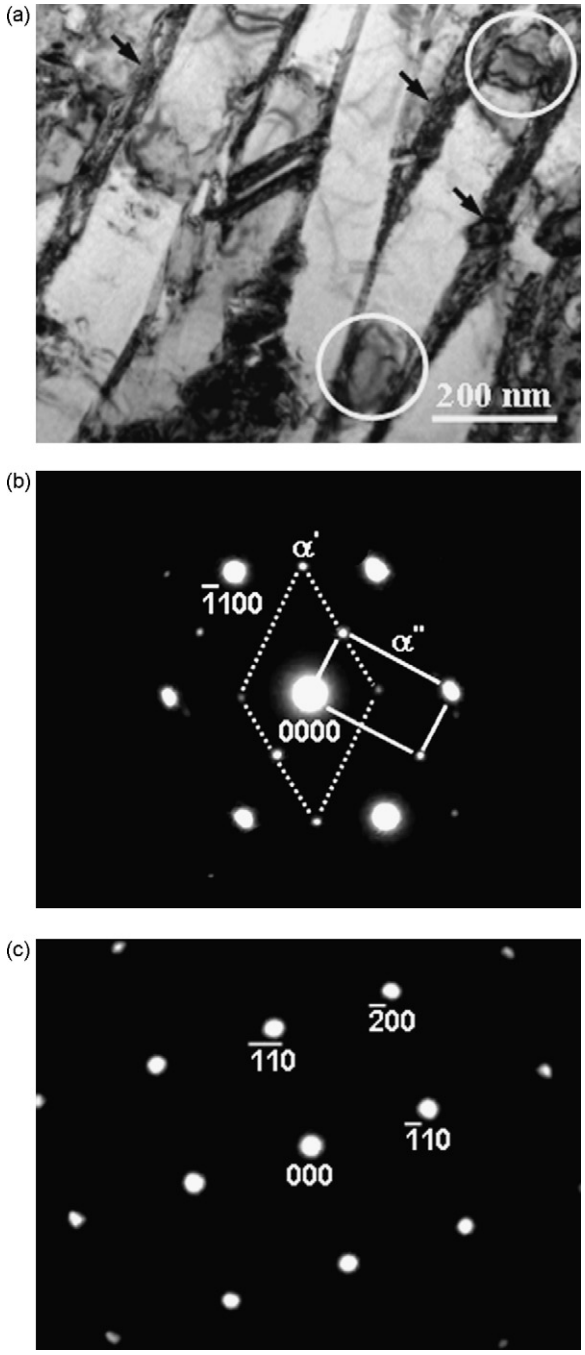

Fig. 3. TEM micrographs of the Ti-5111 alloy sample underwent solution-treated at 890 °C for 30 min: (a) BF, (b) a [0 0 0 1] SAEDP taken from the matrix in (a), and (c) a [1 0 0] SAEDP taken from the residual phase, which was marked white circle region in (a).

plates are usually densely populated with dislocations [26]. Therefore, it is determined that the microstructure of the investigated alloy solution-treated at 860 °C for 30 min comprised (α + α′ + β) phases.

Fig. 3 presents the TEM micrographs of the alloy solution-treated at 890 °C for 30 min. The BF image reveals not only lath-like precipitate (white regions) and acicular precipitate (as indicated by arrows) but also residual phase (as marked by the white circle) in the matrix, as shown in Fig. 3(a). Fig. 3(b) depicts a [0 0 0 1] SAEDP taken from the matrix in Fig. 3(a). In addition to the reflection spots of the α phase, the SAEDP includes two types of superlattice spots. These superlattice spots were the α′ and α″ martensites having an HCP structure and an orthorhombic structure, respectively [14]. The α″ martensite is also a dislocation-type martensite. Fig. 3(c) shows a [1 0 0] SAEDP taken from the residual phase marked with the white circle in Fig. 3(a). The pattern indicates that the residual phase is the β phase with a BCC structure [25]. This characteristic was also detected in the alloy solution-treated at 920 °C. Thus, during solution treatment at 890–920 °C, the Ti-5111 alloy became a mixture of α, α′, α″, and residual β phases.

When the temperature was increased to 960 °C, the macrostructure of the investigated alloy was essentially a single-phase structure. Electron microscopy indicated a phase transition occurred in the matrix. Fig. 4(a) is an SEM image taken from the

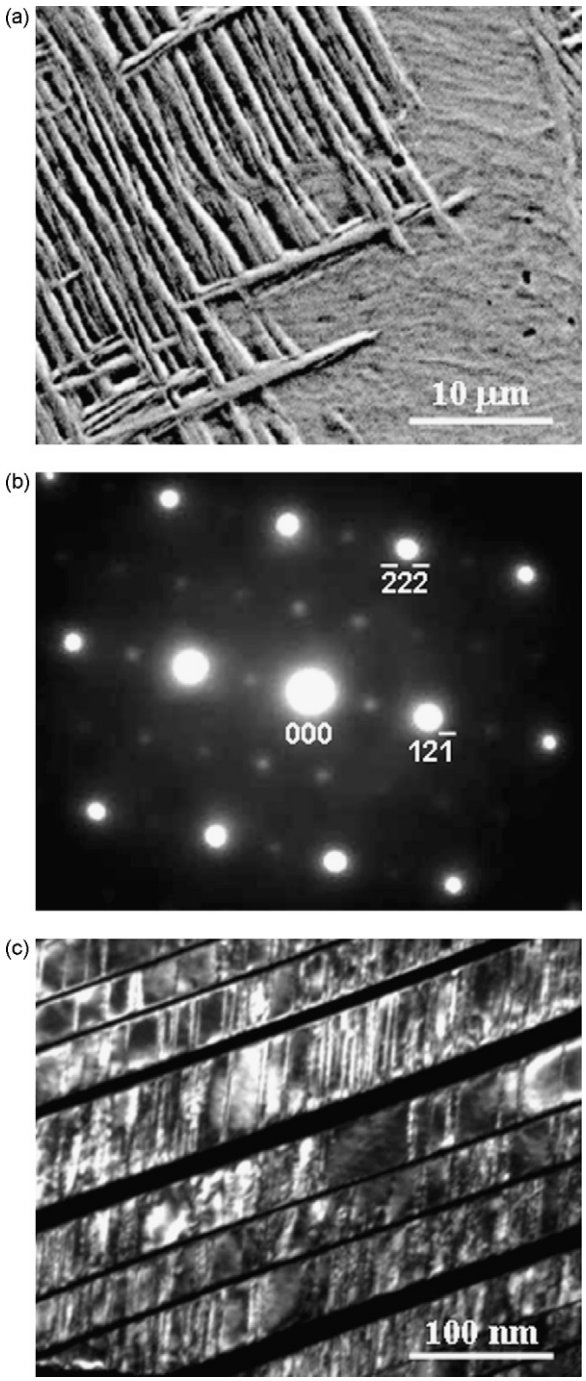

Fig. 4. Electron micrographs of the Ti-5111 alloy sample underwent solution-treated at 960 °C for 30 min: (a) SEM image, (b) a [$\bar{1}$ 2 3] SAEDP taken from a mixed region covering the acicular precipitate and the matrix phase in (a), and (c) the α′ martensite DF.

matrix of the alloy in Fig. 1(f); clearly, acicular precipitates formed in the matrix. Fig. 4(b) shows a [$\bar{1}$ 2 3] SAEDP taken from a mixed region covering acicular precipitate and matrix phase in Fig. 4(a). The figure reveals that the matrix was β phase with BCC structure [25]. In addition to the β phase spots, satellite spots coexist in the SAEDP. These satellite spots were identified as α′ martensite. However, large (1 $\bar{1}$ 0 0) twins were observed within the α′ martensite, as illustrated in Fig. 4(c). Compared to that of observed in Fig. 2, the feature demonstrates that it belongs to a twin-type martensite [26]. Hence, the microstructure of the alloy solution-treated at 960 °C had (α′ + β) phases. As mentioned above, when the investigated alloy underwent solution treatment at temperatures between 800 and 960 °C, the phase transformation sequence was found to be (α + β) → (α + α′ + β) → (α + α′ + α″ + residual β) → (α′ + β).

Table 1
The chemical compositions of the α′ martensite of the Ti-5111 alloy solution-treated at 860 and 960 °C, respectively.

Solution treatment	Phase	Chemical composition (wt.%)		
		Ti	Al	Sn
860 °C–30 min	α′ martensite	Bal.	4.53	1.05
960 °C–30 min	α′ martensite	Bal.	8.60	1.18

The above observations are now discussed. When the Ti-5111 alloy was solution-treated at 860 °C for 30 min, α′ martensite formed in the α matrix. This result strongly suggests that the Ms of the Ti-5111 alloy is nearly 860 °C. The Ms of Ti-5111 alloy is lower than that of Ti–6Al–4V alloy [27]. It is well known that α′ martensite plays an important role in increasing the strengths of duplex Ti alloys [4,26,27]. Peng et al. [4] pointed out that α′ martensite not only increases the tensile strength but also enhances the damping capacity of an alloy. Therefore, it is expected that the formation of α′ martensite promotes the mechanical properties of Ti-5111 alloy.

When the investigated alloy underwent solution treatment at temperatures between 860 and 920 °C, the phase transformation sequence was found to be (α + α′ + β) → (α + α′ + α″ + residual β). Paradkar et al. [28] reported that the athermal decomposition of β during quenching leads to the formation of α′ hexagonal martensite in alloys lean in β stabilizers and α″ orthorhombic martensite in alloys with higher levels of β stabilizers. An example is the Ti–Mo system [29,30]. The β phase transforms to α′ phase in Ti–Mo alloys containing less than 4 wt.% Mo and α″ phase in alloys containing 4–8 wt.% Mo during quenching. A similar effect is observed for Ti–4Al–4Mo–2Sn–0.5Si alloy [31]. In the present sturdy, the β stabilizer content (i.e., the Fe and Cr content in the investigated alloy) is about 2 wt.%, which is less than the range for the formation of α″ phase. However, Paradkar et al. [28] pointed out that the slow cooling of the alloy leads to the formation of equilibrium phases in both the β and α + β regions, whereas rapid cooling (water quenching) results in the transformation of the retained β phase to the α″ phase. Therefore, it is deduced that the cooling rate plays an important role in driving the transformation of the retained β phase to α″ phase in the Ti-5111 alloy solution-treated at temperatures between 860 and 920 °C.

Moreover, an α → β structure transition was observed in the matrix of the alloy solution-treated at 960 °C. This feature demonstrates that the β transus temperature of the Ti-5111 alloy is approximately 960 °C. The β transus determined from metallographic observations is in good agreement with the TEM identifications and confirms that there is an approximate 30–50 °C difference between Ti-5111 alloy and Ti–6Al–4V alloy (1000 ± 14 °C) [32,33]. In applications, the β transus is an important parameter in the thermomechanical processing of Ti alloys because entirely different microstructures are obtained depending on whether the alloy is processed above or below this temperature [32].

Table 1 presents quantitatively the chemical compositions of α′ martensite of Ti-5111 alloys solution-treated at 860 and 960 °C. Basically, the chemical compositions of α′ martensite in both specimens consist of α-stabilizing alloying elements (i.e., Al and Sn). However, with the temperature increasing to 960 °C, it was found that the concentration of Al in α′ martensite is significantly greater than that in the alloy solution-treated at 860 °C for 30 min. The result reveals that the concentration of Al in the α′ martensite plays a crucial role in the formation of the twin-type martensite. Finally, it is worth noting that aging treatment must be further studied

to better understand the microstructure transitional behavior of Ti–5Al–1Sn–1Fe–1Cr alloy.

4. Conclusions

The microstructure of the investigated alloy solution-treated at 860 °C for 30 min comprised ($\alpha + \alpha' + \beta$) phases. The α' martensite had an HCP structure and lattice parameters $a = 2.93$ nm and $c = 4.66$ nm; it is a dislocation-type martensite. As the temperature increased from 890 to 920 °C, not only lath-like α' martensite but also acicular α'' martensite and residual β phase were formed in the matrix. The α'' martensite was identified as having an orthorhombic structure. Above 960 °C, the microstructure of the investigated alloy revealed a β phase with α' martensite. The α' martensite was a twin-type martensite. It was found that the concentration of Al in the α' martensite plays a crucial role in the formation of the twin-type martensite.

Acknowledgements

The authors would like to thank the Center of Excellence for Clinical Trial and Research in Neurology and Neurosurgery, Taipei Medical University-Wan Fang Hospital for financially supporting this research under contract No. DOH99-TDB-111-003, and supported partly by Biomate Medical Devices Technology Co., Ltd.

References

[1] S. Kumar, T.S.N. Sankara Narayanan, J. Alloys Compd. 479 (2009) 699.
[2] T.C. Niemeyer, C.R. Grandini, L.M.C. Pinto, A.C.D. Angelo, S.G. Schneider, J. Alloys Compd. 476 (2009) 172.
[3] J.H. Han, D.H. Park, C.W. Bang, S. Yi, W.H. Lee, K.B. Kim, J. Alloys Compd. 483 (2009) 44.
[4] P.W. Peng, K.L. Ou, C.Y. Chao, Y.N. Pan, C.H. Wang, J. Alloys Compd. 490 (2010) 661.
[5] Z.G. Fan, H. Jiang, X.G. Sun, J. Song, X.N. Zhang, C.Y. Xie, Mater. Sci. Eng. A 527 (2009) 45.
[6] Y.B. Wang, Y.F. Zheng, Mater. Lett. 63 (2009) 1293.
[7] C.F. Huang, H.C. Cheng, C.M. Liu, C.C. Chen, K.L. Ou, J. Alloys Compd. 476 (2009) 683.
[8] W.A. Badawy, A.M. Fathi, R.M. El-Sherief, S.A. Fadl-Allah, J. Alloys Compd. 475 (2009) 911.
[9] D.Q. Wei, Y. Zhou, Appl. Surf. Sci. 255 (2009) 6232.
[10] M. Long, H.J. Rack, Biomaterials 19 (1998) 1621.
[11] M. Niinomi, Biomaterials 24 (2003) 2673.
[12] L.Q. Wang, W.J. Lu, J.I. Qin, F. Zhang, D. Zhang, J. Alloys Compd. 469 (2009) 512.
[13] L.J. Xu, Y.Y. Chen, Z.G. Liu, F.T. Kong, J. Alloys Compd. 453 (2008) 320.
[14] Y.L. Zhou, M. Niinomi, J. Alloys Compd. 466 (2008) 535.
[15] C.N. Elias, J.H.C. Lima, R. Valiev, M.A. Meyers, J. Miner. Met. Mater. Soc. 60 (2008) 46.
[16] M. Niinomi, Sci. Technol. Adv. Mater. 4 (2003) 445.
[17] S.R. Paital, N.B. Dahotre, Mater. Sci. Eng. R 66 (2009) 1.
[18] X. Liu, P.K. Chub, C. Ding, Mater. Sci. Eng. R 47 (2004) 49.
[19] Y.Z. Zhan, X.J. Zhang, J. Hu, Q.H. Guo, Y. Du, J. Alloys Compd. 479 (2009) 246.
[20] D.B. Lee, K.B. Park, H.W. Jeong, S.E. Kim, Mater. Sci. Eng. A 328 (2002) 161.
[21] R.P. Siqueira, H.R.Z. Sandim, A.O.F. Hayama, V.A.R. Henriques, J. Alloys Compd. 476 (2009) 130.
[22] S.C. Huang, E.L. Hall, Metall. Trans. A 22A (1991) 2619.
[23] H.C. Hsu, S.C. Wu, Y.S. Hong, W.F. Ho, J. Alloys Compd. 479 (2009) 390.
[24] F. Karimzadeh, M. Heidarbeigy, A. Saatchi, J. Mater. Process. Technol. 206 (2008) 388.
[25] B.H. Choe, S.K. Shin, Y.O. Kim, Y.T. Hyun, S.E. Kim, Y.T. Lee, Met. Mater. Int. 11 (5) (2005) 365.
[26] J.M. Manero, F.J. Gil, J.A. Planell, Acta Mater. 48 (2000) 3353.
[27] H. Fujii, Mater. Sci. Eng. A 243 (1998) 103.
[28] A.G. Paradkar, V.K. Varma, V. Joshi, T.K. Nandy, A.K. Gogia, S.V. Kamat, B.P. Kashyap, Metall. Trans. A 33A (2002) 2763–2766.
[29] M.J. Blackburn, J.A. Feeney, J. Inst. Met. 99 (1971) 132–134.
[30] R. Davis, H.M. Flower, D.R.F. West, J. Mater. Sci. 14 (1979) 712–722.
[31] K.K. Kharia, H.J. Rack, Metall. Trans. A 32A (2001) 671–679.
[32] S. Tamirisakandala, R.B. Bhat, D.B. Miracle, S. Boddapati, R. Bordia, R. Vanover, V.K. Vasudevan, Scripta Mater. 53 (2005) 217.
[33] R. Ding, Z.X. Guo, Mater. Sci. Eng. A 365 (2004) 172.